ORIGINAL PAPER

Development and characterization of biopolymer electrolyte based on gellan gum (GG) with lithium chloride (LiCl) for the application of electrochemical devices

S. Aafrin Hazaana[1,2] · Ancemma Joseph[1] · S. Selvasekarapandian[2,3] ·
R. Meera Naachiyar[1,2] · M. Vengadesh Krishna[2,4] · N. Muniraj Vignesh[2,5]

Abstract

The biopolymer electrolyte based on gellan gum with various concentrations of lithium chloride salt has been prepared using solution casting technique and optimized with high ionic conductivity of 4.08×10^{-3} S cm^{-1} for the composition of 1 g gellan gum + 1.2 M wt% of LiCl using AC impedance analysis. XRD has been used to study the crystalline/amorphous nature of the prepared membrane. The complex formation between the polymer and the salt is analyzed using FTIR technique. DSC analysis has been done to evaluate the glass transition temperature of the prepared electrolytes. Transference number measurement was done to confirm that the conduction is due to cations. CV analysis was done to measure the cyclic stability of the prepared membrane which shows an adequate result by reciprocating the pattern for 50 cycles. Primary lithium-ion conducting battery is constructed using highest lithium-ion conducting membrane. It shows an open circuit voltage of 1.88 V.

Keywords Gellan gum · Biopolymer electrolyte · AC impedance analysis · Lithium-ion conducting battery

✉ S. Selvasekarapandian
  sekarapandian@rediffmail.com

1   Fatima College, Research Center of Physics, Madurai, Tamil Nadu 625018, India

2   Materials Research Center, Coimbatore, Tamil Nadu 641045, India

3   Department of Physics, Bharathiar University, Coimbatore, Tamil Nadu 641046, India

4   Department of Chemistry, Bharathiar University, Coimbatore, Tamil Nadu 641046, India

5   Department of Physics, Mannar Thirumalai Naicker College, Madurai, Tamil Nadu 625004, India

Introduction

Energy crisis due to the reduction of naturally available fossil fuels (based on their large usage) and the demand toward the development of energy storing electrochemical devices like batteries, fuel cells, etc., leads to the evolution of polymer electrolytes which plays a major role in the fabrication of batteries. Among few promising electrochemical devices, lithium-ion batteries attracted tremendous technological attention worldwide as lithium is one of the lightest metals (equivalent weight: 6.94 g mol^{-1}). They relatively have many applications toward portable electronic devices like watches, camera, mobile phones, laptops, tablets, etc., owing to their high energy density and design flexibility [1].

As liquid electrolytes show high ionic conductivity than the solid electrolytes, many works have been carried out in this field. Though they show better ionic conductivity, few issues like leakage, corrosion, inflammability at high temperatures [2] and growth of metal dendrites from anode to cathode through the electrolyte medium at the time of multiple cycling (charge–discharge) in liquid electrolytes may lead to internal short circuit in the batteries [3]. Overcoming these issues, the solid polymer electrolyte research has proved to be very advantageous with better mechanical and thermal stability, easy synthesis method, no leakage, flexibility, lightweight, safety, transparent with glassy appearance, long lasting capacity that can be utilized [2].

Solid polymer electrolytes (SPE) have two different varieties like synthetic and natural polymers. When compared to few petroleum/chemical-based synthetic polymers, naturally available biopolymers are cost efficient, abundant, biodegradable and less toxic in nature [4]. They also exhibit some gainful features like better ionic conductivity, compatibility with the electrodes, eco-friendly and ease availability [5].

Biopolymers are the diverse set of polysaccharides, proteins, lipids, poly-phenols, etc., produced by the fungi, bacteria, plants and animals [6]. Extensive research has been carried out with biopolymers like agar–agar [5], variety of carrageenans [7, 8], starch [9], cellulose acetate [10], alginate [11], pectin [12], etc., acting as host matrix in the studies of electrolytes owing to versatile electrochemical device applications.

Among variety of biopolymers, gellan gum (GG), also known as Phytagel/Gel-rite/Gelzen [13], is a type of polysaccharide which is composed of α-L-rhamnose, β-D-glucuronic acid and β-D-glucose in the ratio of 1:1:2 (Fig. 1a). It is obtained by the fermentation of a species named *Pseudomonas elodea* consisting of a complex tetrasaccharide repeating unit [14] and has been chosen as a host matrix for the
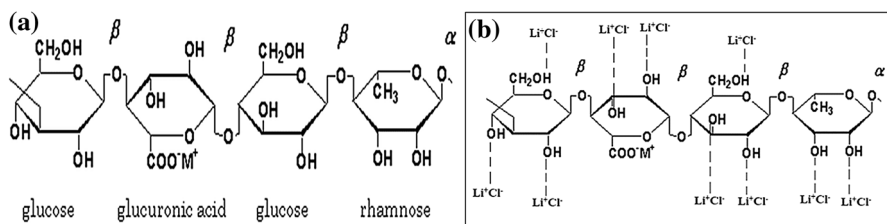
Fig. 1 a Chemical structure of gellan gum and **b** possible interaction of LiCl with the polymer (gellan gum)

preparation of an electrolyte. GG has been utilized much in the field of medicinal applications like ophthalmology for the advancement of lenses having drug-delivery properties, etc., and also as a stabilizer, thickener, gelling agent in foods due to their harmless nature to humans [15]. The distinctive properties of GG are its low viscosity nature, glassy appearance (transparent), high thermal stability up to 120 °C and thermal reversibility (exposing reverse property in heating and cooling) [16]. The reason for choosing GG in our study is it contains good amount of polar groups to which cation of any salt could be attached to increase the conductivity.

Few works have been reported on the preparation of GG-based biopolymer electrolytes (BPEs) which are incorporated with different salts providing ion conduction. I.S.M Noor et al. prepared biopolymer electrolyte with $GG/LiCF_3SO_3$ showing highest conductivity in the range of 5.4×10^{-4} S cm^{-1} at ambient temperature [15], S.R Majid et al. reported maximum conductivity of 5.6×10^{-6} S cm^{-1} at 303 K and 1.6×10^{-4} S cm^{-1} at 373 K for $GG/PVP/LiClO_4$ electrolyte prepared [17]. There are few methods such as usage of plasticizers [18] and appending of inorganic fillers [19] to enhance the ionic conductivity in the electrolytes.

Earlier research work of gellan gum with lithium salts shows only conductivity in the range of 10^{-4} S cm^{-1} ($GG/LiCF_3SO_3$) and 10^{-6} S cm^{-1} ($GG/PVP/LiClO_4$). Our aim is to develop lithium electrolyte using gellan gum and LiCl (lithium chloride is easy to dissociate in a solvent, as the chlorine ions are weakly bonded to lithium ions in contrast to other ionic salts) [20].

This paper deals with the preparation of lithium-ion (Li-ion) conducting electrolytes using GG with different concentrations of LiCl by solution casting technique. The synthesized electrolytes undergo various characterization techniques like X-ray diffraction (XRD), Fourier transform infrared (FTIR) spectroscopy, AC impedance analysis, differential scanning calorimetry (DSC) and transference number measurement to investigate its structural, chemical, electrical and thermal properties. Then, lithium-ion conducting primary battery has been constructed using highest lithium-ion conducting electrolyte.

Experimental section

Materials

Biopolymer, gellan gum (Sisco Research Laboratories Pvt. Ltd) with molecular weight—500 kDa, gelling temperature—35 to 40 °C and lithium chloride (Thomas Baker Chemicals Pvt. Ltd) with molecular weight—42.4 g/mol are used as raw materials with double distilled water as solvent for the preparation of BPE.

Preparation

Solid BPEs based on gellan gum with various compositions (molecular weight percentage—M wt%) of lithium chloride have been synthesized using solution casting technique. 1 g gellan gum was added pinch by pinch in the double distilled water

maintained under the temperature of 80–90 °C and undergoes vigorous magnetic stirring to obtain the clear viscous solution. After complete dissolution of the polymer, different compositions (0.6, 0.9, 1.2 and 1.3 M wt%) of LiCl which is dissolved in warm water were added and stirred for another 1 h to obtain the homogeneous mixture. The resulting solution was poured in a polypropylene petri dish placed in a hot plate maintained with the fixed temperature of 40 °C and permitted to evaporate for 12 h. Finally, the obtained transparent and flexible solid BPEs (film) with thickness ranging from 0.02 to 0.03 cm were obtained.

Characterization techniques

X-ray diffraction

XRD measurements are done to analyze the crystalline/amorphous nature of the prepared samples using Philips X'Pert PRO diffractometer with Cu-Kα radiation source in the wavelength of 1.54 Å and the angle range (2θ) is varied between 5° and 80° at the scanning speed of 10 °/min in ambient temperature [21]

Fourier transform infrared spectroscopy

FTIR analysis was carried out with the SHIMADZU–IR Affinity-1 Spectrometer in the transmission mode within the spectral range 500–4000 cm^{-1} in the resolution of 1 cm^{-1} at room temperature and the results were obtained through ATR method. [21]

Differential scanning calorimetry

The thermal studies were done by differential scanning calorimetric analysis using DSC Q20 V24.11 Build 124 with the temperature ranging from 20 to 200 °C under nitrogen atmosphere at the heating rate of 10°/min [4]

AC impedance technique

The ionic conductivity of the prepared electrolyte has been calculated by measuring impedance using HIOKI-3532 LCR Hi-Tester analyzer interfaced to a computer in the frequency range of 42 Hz–5 MHz at room temperature. The bulk conductivity has been calculated from Nyquist plots using Boukamp software [31].

Transference number measurement

Wagner's polarization technique

The DC polarization method was performed to identify the nature of charge carriers in the electrolyte sandwiched between two stainless steel electrodes by supplying a

fixed DC voltage of 1.5 V and monitoring the DC current as a function of time [36, 38]

Evan's polarization technique

The transference number of cation is measured by supplying a small amount of DC voltage along with AC impedance analysis for the cell arranged with the configuration of silver electrode ‖ 1 g GG + 1.2 M wt% of LiCl (highest ionic conductivity optimized sample) ‖ silver electrode [36, 38].

Cyclic voltammetry

The electrochemical cycling stability for the high ion conducting membrane has been analyzed via two electrode system using CHI600C Series electrochemical analyzer with the potential range (V) of − 1 V to + 1 V and scan rate of 0.1 V/s [30].

Battery construction

Fabrication of Li-ion conducting battery

Preparation of cathode Cathode is prepared by grinding lead oxide (PbO_2), vanadium pentoxide (V_2O_5), graphite (C) and a pinch of highest conducting polymer electrolyte (1 g GG + 1.2 M wt% of LiCl) with the proper ratio of 8:2:1:0.5 and the grinded mixture was given hydraulic pressure to form a thin pellet [4].

Preparation of anode Anode is composed with the suitable ratio of zinc dust powder, $ZnSO_4 \cdot 7H_2O$ and graphite powder (C) as 3:1:1 and grinded well. Then, the grinded composition is made into a thin pellet using a hydraulic press machine [4].

Construction of battery Li^+-ion conducting battery has been constructed by sandwiching the prepared anode and cathode pellets along with the highest ion conducting electrolyte in the configuration of $Zn + ZnSO_4 \cdot 7H_2O + C$ (as anode)‖Li^+-ion highest conducting membrane (as electrolyte)‖$PbO_2 + V_2O_5 + C$ + electrolyte (as cathode) under ambient temperature. The open circuit voltage (OCV) and the discharge characteristics were observed.

Results and discussion

X-ray diffraction

X-ray diffraction is a technique used to determine the crystalline/amorphous nature of the prepared BPE. The XRD patterns of pure GG and the gellan gum incorporated with LiCl are depicted in Fig. 2a (i)–(v). From Fig. 2a (i), the
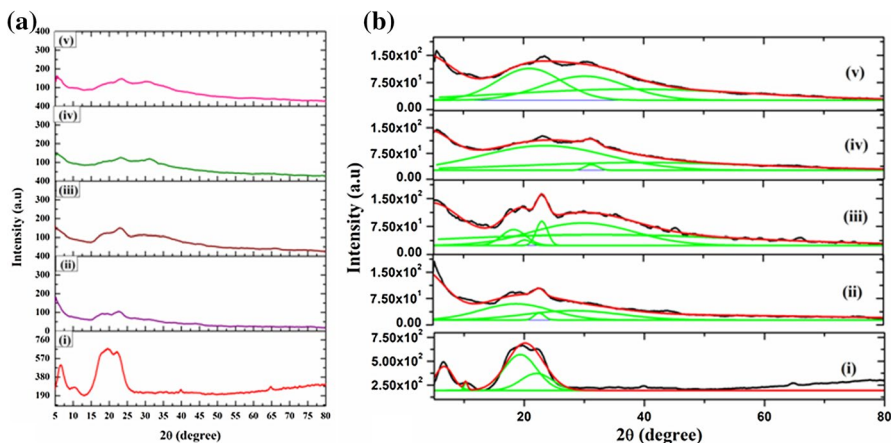
Fig. 2 **a** XRD and **b** deconvoluted patterns of (*i*) pure gellan gum (1 g), (*ii*) 1 g GG + 0.6 M wt% of LiCl, (*iii*) 1 g GG + 0.9 M wt% of LiCl, (*iv*) 1 g GG + 1.2 M wt% of LiCl and (*v*) 1 g GG + 1.3 M wt% of LiCl

semicrystalline peaks of pure gellan gum are observed at angle of $2\theta = 6°$, $10°$, $19°$ and $22°$, which are in accordance with earlier report [21].

Consecutively, by analyzing, it is found from Fig. 2a (ii)–(v), that the intensity of diffracted peaks decreases and broadness of the peaks increases with the addition of LiCl in the prepared electrolytes. Moreover, it is to be noted that the peaks observed at $2\theta = 6°$ and $10°$ in pure GG [Fig. 2a (i)] have been suppressed in 1 g GG + 0.6 M wt% of LiCl, 1 g GG + 0.9 M wt% of LiCl and 1 g GG + 1.2 M wt% of LiCl, and the membrane 1 g GG + 1.3 M wt% of LiCl shows slight increase in intensity of the peak at $2\theta = 10°$, respectively. Then, the peaks at $2\theta = 19°$ and $22°$ in 1 g GG + 0.6 M wt% of LiCl, 1 g GG + 0.9 M wt% of LiCl and 1 g GG + 1.2 M wt% of LiCl have become prominently less in intensity with the increase in its broadness when compared to pure GG, which confirms the increase in amorphous nature of the membranes by the addition of salt. Then, the XRD pattern of the biopolymer 1 g GG + 1.3 M wt% of LiCl shows modest increase in intensity at the peaks $17°$, $18°$ and $23°$, respectively. Here, it is observed that on further addition of salt (i.e., above 1.2 M wt% of LiCl), the membrane with the composition of 1 g GG + 1.3 M wt% of LiCl shows an increase in the intensity with decrease in broadness of the peak when compared to other salt added membranes, which assures the increase in crystalline nature of the sample due to the aggregation/accumulation of the ions. It is seen from the XRD patterns of all samples that 1 g GG + 1.2 M wt% of LiCl membrane has got high amorphous nature.

The results provided for the intensity and broadness of the peaks are in accordance with the criteria reported by Hodge et al. [22]. It is to be noted that the peaks due to LiCl are absent at all polymer membranes with salt indicating complete dissociation of salt. The crystalline percentage for the samples prepared has also been calculated from the formula provided below using deconvoluted XRD patterns,

Table 1 Crystalline percentage for the prepared biopolymer electrolytes

Polymer composition	Percentage of crystallinity (%C)
1 g GG (Pure)	33.76
1 g GG + 0.6 M wt% of LiCl	8.84
1 g GG + 0.9 M wt% of LiCl	8.22
1 g GG + 1.2 M wt% of LiCl	7.61
1 g GG + 1.3 M wt% of LiCl	7.67

Table 2 Vibrational peaks with its spectral band assignments of all the prepared biopolymer electrolytes

| Pure gellan gum (cm^{-1})	1 g GG + (X) M wt% of LiCl (cm^{-1})				Assignments	References
	X = 0.6	X = 0.9	X = 1.2	X = 1.3		
3289	3382	3370	3358	3370	O–H stretching	[21]
2919	2927	2924	2922	2922	CH$_2$ asymmetric stretching	[23, 24]
1639	1616	1628	1627	1630	Glycosidic bond	[25, 26]
1431	1420	1432	1434	1437	C–C stretching (in ring)	[13]
1039	1038	1039	1042	1051	C–O–C stretching of pyranose ring	[27]

$$\text{Percentage of crystallinity}(\%C) = \frac{\text{Area under crystalline region}}{\text{Total area of the peak}} \times 100\%.$$

Table 1 illustrates the crystalline percentage calculated for the prepared BPEs and Fig. 2b depicts the deconvoluted XRD graph patterns. From Table 1, it is observed that the crystalline percentage calculated for pure GG is 33.76% [21] which is enormously high when compared to the electrolytes incorporated with the salt LiCl (0.6, 0.9, 1.2 and 1.3 M wt% of LiCl). This reveals the concept that percentage of crystallinity decreases with increase in salt concentration. On further analysis, the sample with 1 g GG + 1.2 M wt% of LiCl has been observed with a decreased crystallinity percentage in contrast with other BPEs, indicating the high amorphous nature of the membrane. Further, on addition of salt, an electrolyte with the composition of 1 g GG + 1.3 M wt% of LiCl, results with an increased crystalline percentage due to the formation of clusters.

Fourier transform infrared spectroscopy

Fourier transform infrared (FTIR) spectroscopic analysis is done to confirm the complex formation between gellan gum and the salt (LiCl).

The observed peak position and its assignments are shown in Table 2. FTIR spectrum is shown in Fig. 3. The broad vibrational peak at 3289 cm^{-1} in pure GG is attributed to O–H stretch (hydroxyl group) and this OH vibration has been shifted to 3382, 3370, 3358 and 3370 cm^{-1} for 1 g GG + 0.6 M wt% of LiCl, 1 g GG + 0.9 M wt% of LiCl, 1 g GG + 1.2 M wt% of LiCl and 1 g GG + 1.3 M wt% of
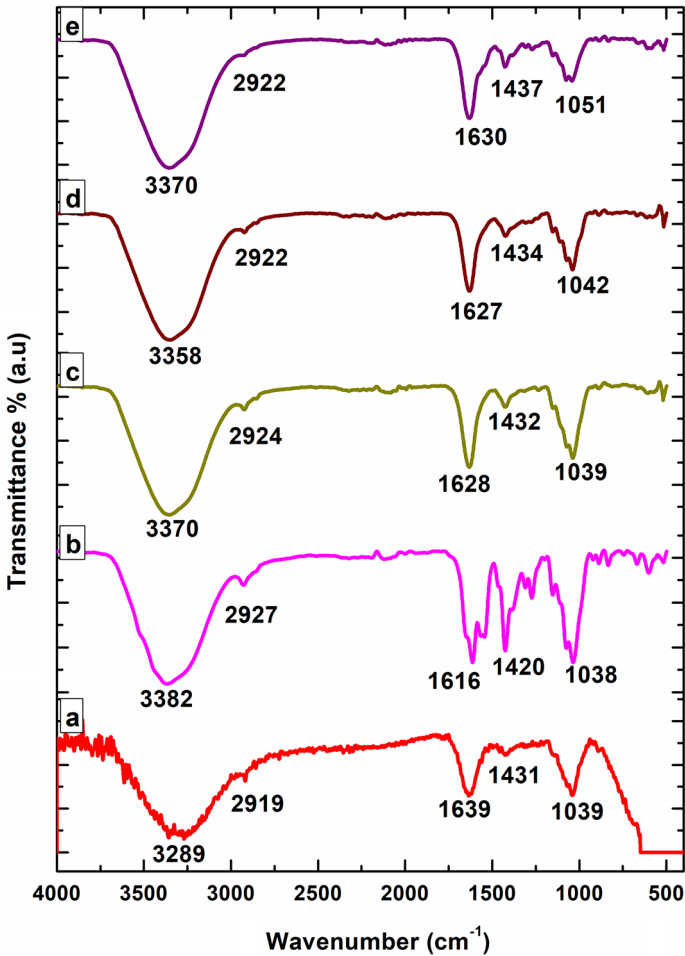
Fig. 3 FTIR spectra of **a** pure gellan gum (1 g), **b** 1 g GG + 0.6 M wt% of LiCl, **c** 1 g GG + 0.9 M wt% of LiCl, **d** 1 g GG + 1.2 M wt% of LiCl and **e** 1 g GG + 1.3 M wt% of LiCl

LiCl, respectively [21]. The increase in frequency of OH group is due to the interaction between the oxygen of OH group and Li^+ of lithium chloride. This confirmed the complex formation between the Li^+ and the polymer, gellan gum. The vibrational peak at 2919 cm^{-1} in pure GG is representing to CH_2 asymmetric stretching and gets shifted to 2927, 2924, 2922 and 2922 cm^{-1} for the membrane with the composition of 1 g GG + 0.6 M wt% of LiCl, 1 g GG + 0.9 M wt% of LiCl, 1 g GG + 1.2 M wt% of LiCl and 1 g GG + 1.3 M wt% of LiCl, respectively [23, 24]. The peak at 1639 cm^{-1} of pure GG attributed to glycosidic bond has been shifted to lower wave numbers for the compositions 1 g GG + 0.6 M wt% of LiCl (1616 cm^{-1}), 1 g GG + 0.9 M wt% of LiCl (1628 cm^{-1}), 1 g GG + 1.2 M wt% of LiCl (1627 cm^{-1}) and 1 g GG + 1.3 M wt% of LiCl (1628 cm^{-1}) [25, 26] whereas the peak 1616 cm^{-1} of 1 g GG + 0.6 M wt% of LiCl gets narrowed down for membranes 1 g

GG + 0.9 M wt% of LiCl, 1 g GG + 1.2 M wt% of LiCl and 1 g GG + 1.3 M wt% of LiCl, respectively. The peak corresponding to C–C stretching (in ring) at 1431 cm^{-1} in pure GG is shifted to 1420, 1432, 1434 and 1437 cm^{-1} for the composition of 1 g GG + 0.6 M wt% of LiCl, 1 g GG + 0.9 M wt% of LiCl, 1 g GG + 1.2 M wt% of LiCl and 1 g GG + 1.3 M wt% of LiCl representing the vibrations of groups with local symmetry encountered in carbohydrates [13]. The common intense band 1039 cm^{-1} in most of all polysaccharides is representing C–O–C stretching of pyranose ring and has been shifted to wave numbers 1038, 1039, 1042 and 1051 cm^{-1} for 1 g GG + 0.6 M wt% of LiCl, 1 g GG + 0.9 M wt% of LiCl, 1 g GG + 1.2 M wt% of LiCl and 1 g GG + 1.3 M wt% of LiCl, respectively [23, 27]. The minor peaks between the wavelength region 1616 to 1038 observed in 1 g GG + 0.6 M wt% of LiCl, have been suppressed in 1 g GG + 0.9 M wt% of LiCl, 1 g GG + 1.2 M wt% of LiCl and 1 g GG + 1.3 M wt% of LiCl, respectively.

The shift in peak position, change in intensity and narrowing of the peaks indicates complex formation between gellan gum and lithium chloride. The possible interaction between gellan gum and lithium chloride is shown in Fig. 1b.

The force constant, k has been calculated using Hooke's formula,

$$v = \frac{1}{2\pi c}\sqrt{\frac{k}{\mu}} \text{ N/cm}$$

where $\mu = \frac{m_1 \times m_2}{m_1 + m_2}$ gives the reduced mass. Table 3 represents the force constant calculated for O–H stretching. It is observed from the table, as the molecular weight percentage of LiCl increases, it is found that force constant also increases. When the force constant increases, bond length decreases. Decrease in bond length leads to increase in vibrational frequency. This confirms the complex formation between the polymer and the salt with bond length variation.

Differential scanning calorimetry

The thermal analysis of the prepared electrolytes is examined using differential scanning calorimetry (DSC) by determining the glass transition temperature (T_g), which represents the transition from glass to rubbery state of the complex matrix.

Table 3 Force constant for O–H stretching

Polymer compositions	O–H stretching	
	Wave number (cm^{-1})	Force constant (N cm^{-1})
Pure GG (1 g)	3289	599.88
1 g GG + 0.6 M wt% of LiCl	3382	634.28
1 g GG + 0.9 M wt% of LiCl	3370	629.79
1 g GG + 1.2 M wt% of LiCl	3358	625.31
1 g GG + 1.3 M wt% of LiCl	3370	629.79

DSC plots of pure gellan gum and the BPEs with increasing salt concentrations are depicted in Fig. 4. The glass transition temperatures obtained for each thermogram are tabulated in Table 4. The glass transition temperature of pure gellan gum is observed as 46.57 °C [21]. In current work, by the addition of salt (0.6 M wt% of LiCl and 0.9 M wt% of LiCl) in an electrolyte, the T_g value has been increased to 55.80 °C and 63.02 °C (refer Table 4) which may be due to strong transient cross-linkage between the polymer (GG) and the salt. Further incorporation of salt to 1.2 M wt% of LiCl, resulted with the glass transition temperature, T_g of 60.49 °C. Even the polymer complex with the composition of 1 g GG+1.2 M wt% of LiCl shows decreased transition temperature in contrast with other samples, it is still not substantiable as it is greater than the T_g value of pure gellan gum. The above-discussed analogous behavior of glass transition temperature for additive salt
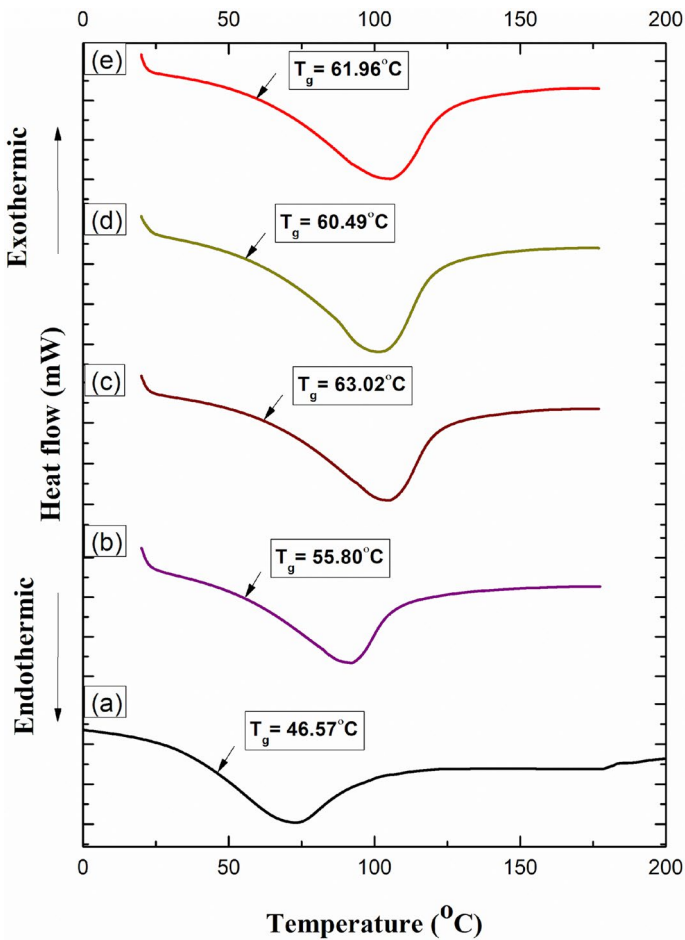
Fig. 4 DSC thermograms of a pure gellan gum (1 g), b 1 g GG+0.6 M wt% of LiCl, c 1 g GG+0.9 M wt% of LiCl, d 1 g GG+1.2 M wt% of LiCl and e 1 g GG+1.3 M wt% of LiCl

Table 4 Glass transition temperature (T_g) of all prepared biopolymer electrolytes

Polymer composition	Glass transition temperature (T_g, °C)
1 g GG (pure)	46.57
1 g GG + 0.6 M wt% of LiCl	55.80
1 g GG + 0.9 M wt% of LiCl	63.02
1 g GG + 1.2 M wt% of LiCl	60.49
1 g GG + 1.3 M wt% of LiCl	61.96

concentration has also been reported by R Chitra et al. for I-Carrageenan with LiCl [4] and L. Sampath Kumar et al., for tamarind seed polysaccharide with $LiCF_3SO_3$ [32]. Subsequently, the complex with increased salt concentration of 1.3 M wt% of LiCl has shown slight increase in T_g value as 61.96 °C by the reason of undissociated salt in the polymer matrix leading to the hardness in polymer backbone thus with increasing percentage of crystallinity (confirmed by XRD) [28].

Calculation of crystallinity percentage from DSC

The crystallinity percentage has been calculated from the enthalpy of the DSC curves for the prepared biopolymer electrolytes using the following equation [4]:

$$\% \text{ of crystallinity} = \frac{\Delta H_m}{\Delta H_m^p} \times 100\%$$

where ΔH_m is the enthalpy for the prepared BPEs and ΔH_m^p is the enthalpy for the pure gellan gum.

The enthalpy values are noted from DSC curves. The percentage of crystallinity calculated for the compositions of 1 g GG + 0.6 M wt% of LiCl, 1 g GG + 0.9 M wt% of LiCl, 1 g GG + 1.2 M wt% of LiCl and 1 g GG + 1.3 M wt% of LiCl is 41.3, 27.6, 20.8 and 23.1%, respectively. The value obtained from DSC data is different from XRD data, but the trend of decreasing crystallinity nature, as we increase the salt concentrations follows. Minimum crystallinity is observed for the membrane with the composition of 1 g GG + 1.2 M wt% of LiCl.

AC impedance analysis

Impedance measurement is a technique done to characterize the electrical properties (Ionic conductivity) of the prepared electrolytes. Few factors affecting the ionic conductivity are concentration of ion conducting species, migration of charge carriers and the temperature [29]. In general, the Nyquist plot consists of semicircle in high-frequency region indicating the presence of bulk properties of the electrolyte with resistor and capacitor in parallel combination, whereas the bulk resistor gives information regarding ion migration through the volume of the complex polymer and bulk capacitor specifies the immobile polymer chain [4]. Then, the low-frequency
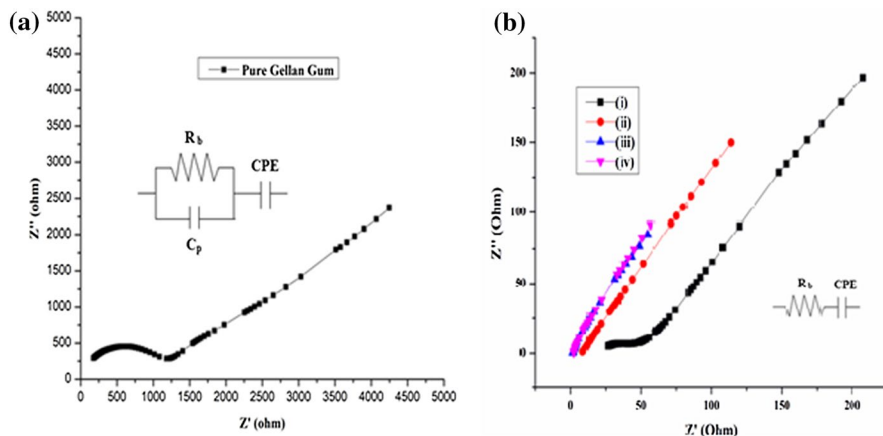
Fig. 5 Nyquist plots of **a** pure gellan gum (1 g) and **b** (*i*) 1 g GG + 0.6 M wt% of LiCl, (*ii*) 1 g GG + 0.9 M wt% of LiCl, (*iii*) 1 g GG + 1.2 M wt% of LiCl and (*iv*) 1 g GG + 1.3 M wt% of LiCl

Table 5 Ionic conductivity and electrochemical impedance spectroscopy parameters for the prepared biopolymer electrolytes

Composition	Conductivity (S cm^{-1})	R_b (Ohm)	CPE (μF)	n (no unit)
1 g GG (pure)	3.07×10^{-7}	1646	30	0.4998
1 g GG + 0.6 M wt% of LiCl	6.90×10^{-5}	5.267	3383	0.1381
1 g GG + 0.9 M wt% of LiCl	6.30×10^{-4}	2.822	128	0.5955
1 g GG + 1.2 M wt% of LiCl	4.08×10^{-3}	1.473	54	0.7849
1 g GG + 1.3 M wt% of LiCl	2.66×10^{-3}	2.127	55	0.7767

inclined spike reveals the adsorption of mobile charge carriers at electrode/electrolyte interface and result with electrical double layer also known as constant phase element (CPE) [30].

Nyquist plots for gellan gum with different concentrations of LiCl illustrated in Fig. 5b show that the high-frequency semicircle vanishes on increasing the concentration of the salt and inclined spike at low-frequency region is alone present indicating the absence of capacitive nature of the electrolyte with the dominance of resistive component and its total conductivity is due to the conduction of ionic charge carriers.

The ionic conductivity of the prepared BPEs can be measured using the formula,

$$\sigma = \frac{l}{AR_b} \ \text{S cm}^{-1}$$

where l is the thickness, R_b is the bulk resistance and A is the known area of the BPE. Bulk resistance (R_b) along with electrochemical impedance spectroscopy (EIS) parameters are obtained from Nyquist plot using EQ software developed by Boukamp [31] (Table 5).

The impedance of constant phase element is represented with the equation [21],

$$Z_{\text{CPE}} = \frac{1}{Q_0(jw)^n}.$$

Here Q_0 and n are frequency independent parameters and n value varies from 0 to 1. If $n=1$, it denotes pure capacitor and if $n=0$, it represents pure resistor. The Resistance (R_b) value of pure GG is 1646 Ω and the R_b value ranges from 5.2 to 2.1 (Ω) for the composition of 1 g GG + various concentrations of LiCl (0.6, 0.9, 1.2 and 1.3 M wt%), respectively. The pure gellan gum gives CPE value of 30 µF and the CPE values for the electrolytes of 1 g gellan gum with various concentrations (0.6, 0.9, 1.2 and 1.3 M wt%) of LiCl are 3383, 128, 54 and 55 µF, respectively. The n value of pure gellan gum is 0.4998 and for the electrolytes with 1 g GG + different concentrations of salt such as 0.6 M wt% of LiCl, 0.9 M wt% of LiCl, 1.2 M wt% of LiCl and 1.3 M wt% of LiCl, the n values are 0.1381, 0.5955, 0.7849 and 0.7767, respectively.

The conductivity values for the prepared BPE listed in Table 5 show the increase in ionic conductivity with the increase in salt concentration. The high ionic conductivity was obtained for the BPE (1 g GG + 1.2 M wt% of LiCl) as 4.08×10^{-3} S cm^{-1} at ambient temperature. This implies that the above-mentioned BPE observed with high conductivity is due to the increase in number of charge carriers, available free volume for movement of ions, increased amorphous nature (confirmed by XRD). Few works based on BPEs with lithium chloride as an additive for better ionic conductivity are Iota-Carrageenan with LiCl showing ionic conductivity of 5.33×10^{-3} S cm^{-1} at room temperature by R.Chitra et al., [4], Pectin/LiClO$_4$ resulting with 5.15×10^{-5} S cm^{-1} ionic conduction at room temperature [30], Tamarind seed polysaccharide with LiCF$_3$SO$_3$ done by L. Sampath Kumar et al., has been optimized with high ionic conductivity of 8.37×10^{-4} S cm^{-1} at ambient temperature [32]. Further, on addition of salt (LiCl), the membrane with the composition of 1 g GG + 1.3 M wt% of LiCl shows decreased ionic conductivity of 2.66×10^{-3} S cm^{-1} which is due to the aggregation of ions in the form of clusters.

Conductance spectra

The frequency-dependent conductance spectra of pure GG (1 g) and various compositions with different weight percentages of LiCl (0.6, 0.9, 1.2, 1.3 M wt%) are clearly represented in Fig. 6. Basically, the spectrum is a combination of three different regions [33]. In the present study, by analyzing Fig. 6 we can conclude that only low-frequency and mid-frequency regions are obtained. The mid-frequency plateau region attributes the tremendous DC conductivity, as the mobility of charge carriers is dominant in this region due to the hopping motion of ions [34]. The value of σ_{dc} can be determined by extrapolating the plateau region to zero frequency (log σ axis). The logarithmic conductivity value obtained for 1 g GG + 1.2 M wt% of LiCl which gives high ionic conductivity is − 2.323. The ionic conductivity calculated by conductance spectra is 4.75×10^{-3} S cm^{-1} which is in resemblance with the bulk conductivity value (4.08×10^{-3} S cm^{-1}) obtained from Nyquist plots.
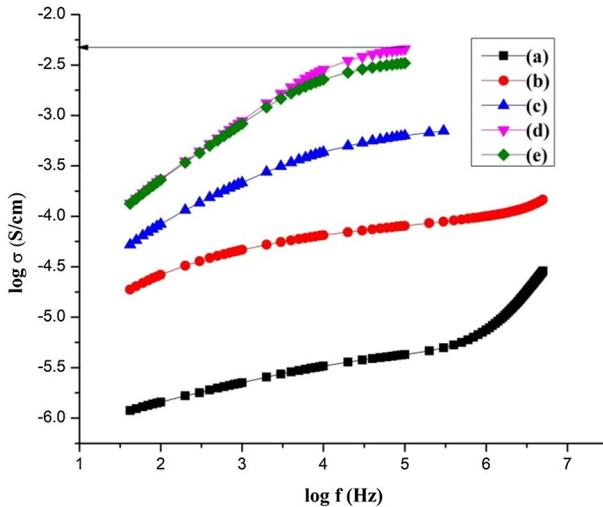
Fig. 6 Conductance spectra of a pure gellan gum (1 g), b 1 g GG + 0.6 M wt% of LiCl, c 1 g GG + 0.9 M wt% of LiCl, d 1 g GG + 1.2 M wt% of LiCl and e 1 g GG + 1.3 M wt% of LiCl

Transference number measurement

Wagner's polarization technique

The transference number measurement carried out by Wagner's polarization technique [35] is done to examine the total ionic (t_+) and electronic (t_-) contribution in the highest conducting BPE (1 g GG + 1.2 M wt% of LiCl).

The method is carried out by placing the membrane showing high conductivity value between two stainless steel electrodes at ambient temperature. Then, a minimal amount of DC voltage is supplied to the cell and the initial current obtained is noted. Then, as the time increases, the cell shows a moderate decrease in the current and becomes stable at a particular time which is measured as final current [36]. Figure 7a depicts the variation in current with the plateau region as a function of time. From Fig. 7a, we can analyze the drop in current with respect to time owing to the polarization effect (i.e., the depletion of ionic and electronic charge carriers). Finally, it attains the depleted state where the current becomes stable with only electronic charge carriers as the ions are completely used [32].

From the measured initial and final current, the total number of ions (t_+) and electrons (t_-) transferring through the electrolyte could be determined using the formula [37],

$$t_+(\text{or})t_{\text{ion}} = \left(I_i - I_f\right)/I_i$$
$$t_-(\text{or})t_{\text{elec}} = I_f/I_i$$

where t_+ total transference number of cation (ions), t_- total transference number of anion (electrons), I_i initial current, I_f final current.

(a)   **(b)**
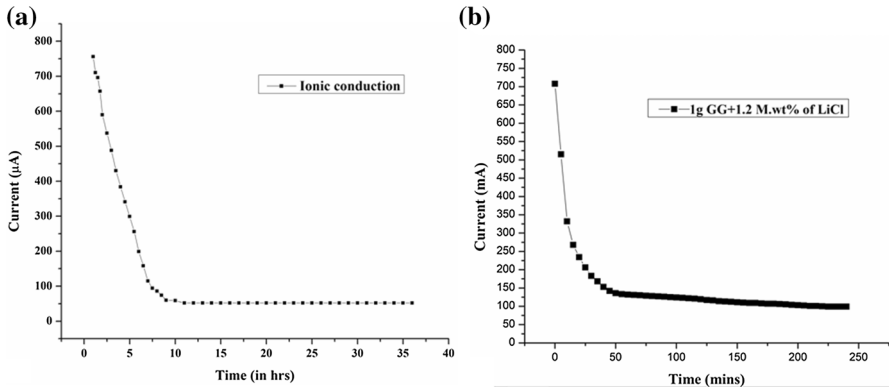
Fig. 7 **a** Variation in DC current with respect to time and **b** current versus time plot for high ion conducting membrane of 1 g GG + 1.2 M wt% of LiCl

The ionic and electronic transference number calculated is 0.93 and 0.07 for an electrolyte (1 g GG + 1.2 M wt% of LiCl) with high optimized conducting value ensuring that the major contribution is due to the ionic charge carriers whereas the electronic charge carriers are considered to be negligible.

Bruce and Vincent method

The cationic transference number (t_+) of the prepared polymer membrane showing high ionic conductivity is evaluated by the combined AC and DC technique of Bruce and Vincent method. In the present study, the electrochemical cell with the configuration of Y(Silver electrode)|YX(Electrolyte)|Y(Silver electrode) has been polarized by applying a small DC voltage (V). The initial (I_o) and final (I_s) steady current values are noted and the current (µA) versus time (mins) plot for the electrolyte with the composition of 1 g GG + 1.2 M wt% of LiCl showing high ionic conductivity is shown in Fig. 7b. Subsequently, AC impedance measurements were also observed to calculate the resistances before (R_o) and after (R_s) polarization of the cell. Figure 8 ascribes the plot of impedance before and after polarization for the cell constructed. The value of cationic transference number (t_{Li^+}) is calculated by [38]

$$t_{Li^+} = \frac{I_s\left(V - I_o R_o\right)}{I_o\left(V - I_s R_s\right)}.$$

The calculated lithium-ion transference number for the prepared BPE of 1 g GG + 1.2 M wt% of LiCl is 0.60, respectively. This shows that the conduction of lithium ion is dominant in the polymer membrane with the composition of 1 g GG + 1.2 M wt% of LiCl. Chitra et al. have reported lithium-ion conduction of 0.55 for 1.0 g i-carrageenan/0.5 wt% of LiClO$_4$ [38] and Arockia Mary et al. have shown 0.58 of lithium-ion transference number for 1 g K-Carrageenan with 0.65 wt% of LiNO$_3$, respectively [36].
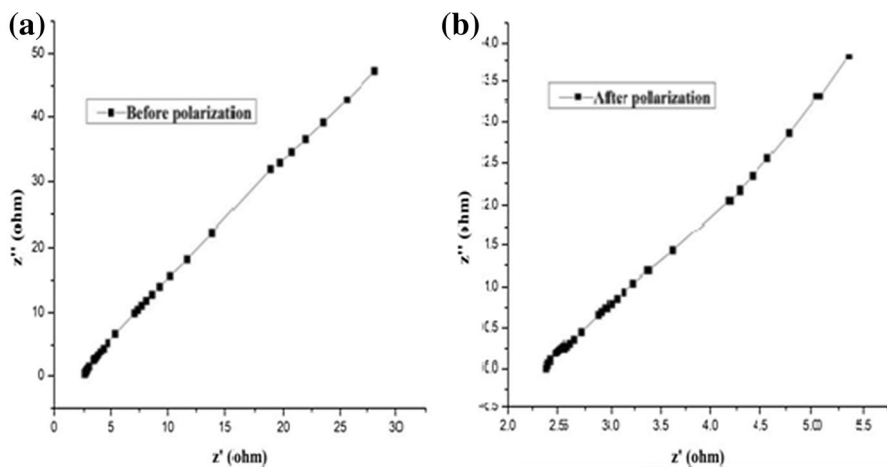
Fig. 8 Impedance plot of **a** 1 g GG + 1.2 M wt% of LiCl before polarization and **b** 1 g GG + 1.2 M wt% of LiCl after polarization

Cyclic voltammetry

In the present work, cycling stability of the prepared highest ion conducting BPE has been analyzed using cyclic voltammetry with the two electrode system. The potential range and the scan rate were fixed within the range of − 1 V to + 1 V and 0.1 Vs^{-1}. The BPE with the composition of 1 g GG + 1.2 M wt% of LiCl producing better ionic conductivity results with an adequate cycling stability for 50 cycles. This CV pattern is reciprocated without much change in its sweep area for each cycle which confirms the reversibility of an electrolyte. Then, the process of redox reaction happens, whereas the oxidation takes place in anode followed by the reduction in cathode. The corresponding CV curves are represented in Fig. 9.

Fabrication of Li-ion conducting battery and its configuration

Solid BPEs prepared with different weight percentages of LiCl were analyzed and the highest Li-ion conducting membrane (1 g GG + 1.2 M wt% of LiCl) is utilized as an electrolyte in the fabrication of Li-ion conducting solid-state battery, whereas the anode and cathode for the battery fabricated are prepared in the form of pellets in an appropriate ratio [27]. Finally, the battery is fabricated by sandwiching the chosen biopolymer electrolyte between the anode and cathode pellets prepared in the configuration of $Zn + ZnSO_4 \cdot 7H_2O + C|1$ g GG + 1.2 M wt% of $LiCl|PbO_2 + V_2O_5 + C + BPE$ [39] and is also represented in Fig. 10 [21].

The reaction of anode and cathode in the fabricated solid-state battery is presented below [21].
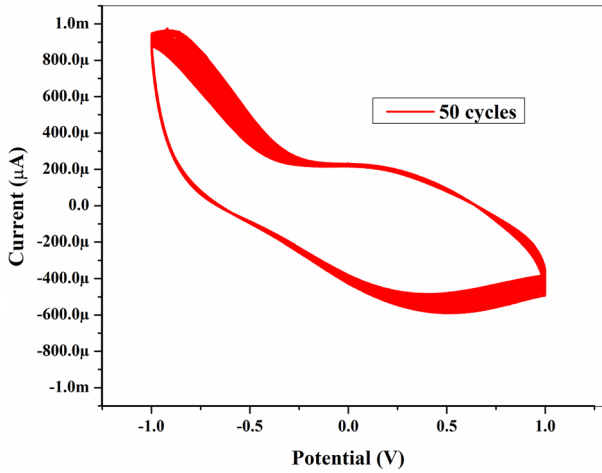
The anode reaction is given as follows:

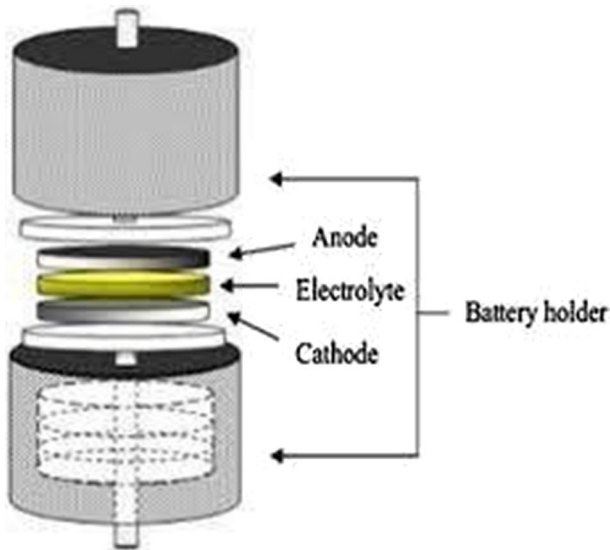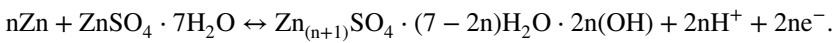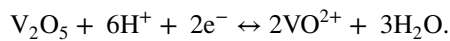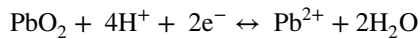**Fig. 9** Characteristics of CV curves for 50 cycles


Fig. 10 Depiction of fabricated solid-state battery

$$nZn + ZnSO_4 \cdot 7H_2O \leftrightarrow Zn_{(n+1)}SO_4 \cdot (7 - 2n)H_2O \cdot 2n(OH) + 2nH^+ + 2ne^-.$$

The cathode reaction is given as follows:

$$PbO_2 + 4H^+ + 2e^- \leftrightarrow Pb^{2+} + 2H_2O$$
$$V_2O_5 + 6H^+ + 2e^- \leftrightarrow 2VO^{2+} + 3H_2O.$$

Now, H^+ ions produced by the anode site repel the Li^+ ions in the BPE to the cathode site by the process of hopping mechanism [40] producing an open circuit voltage (OCV) of 1.88 V which was steadily optimized for 60 h (refer Fig. 11a). Further, on applying a load of 100 KΩ, the voltage drops to 1.79 V and the current drawn is 19 µA whereas the setup is retained for 60 h. Figure 11b depicts the voltage drop analysis with the function of time. M. Premalatha et al. have reported an OCV of 1.63 V for tamarind seed polysaccharide with LiBr [41] and L. Sampath Kumar et al. have studied tamarind seed polysaccharide with $LiCF_3SO_3$ and fabricated a lithium-ion conducting battery with an OCV of 1.85 V [32]. The examined cell parameters are listed in Table 6.

Conclusion

The biopolymer electrolyte based on gellan gum with various concentrations of lithium chloride salt has been prepared using solution casting technique. Using AC impedance analysis, the ionic conductivity has been calculated for all the prepared membranes and the high ionic conductivity was measured as 4.08×10^{-3} S cm^{-1} for the composition of 1 g GG + 1.2 M wt% of LiCl. XRD study reveals the crystalline/amorphous nature of all the membranes, whereas the membrane with the composition of 1 g GG + 1.2 M wt% of LiCl shows high amorphous nature with crystallinity percentage of 7.61%C. The complex formation of polymer and the salt is confirmed by FTIR analysis. DSC analysis has been done and the T_g value was determined for all the prepared BPEs. The membrane with the composition of 1 g GG + 1.2 M wt% of LiCl shows slightly decreased T_g value of 60.49 ℃ when compared to all other salt added BPEs. Transference number measurement was done to authenticate that
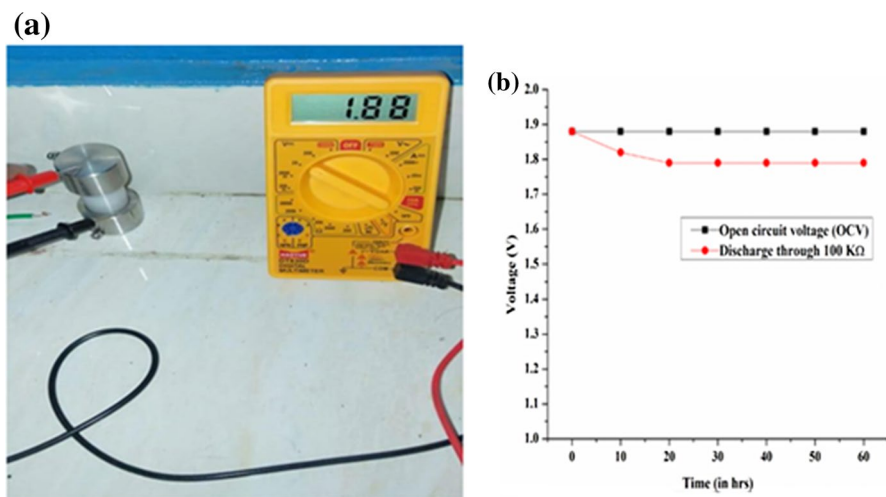
Fig. 11 **a** Open circuit voltage of 1 g GG + 1.2 M wt% of LiCl and **b** plot representing voltage versus time (in h)

Table 6 Important cell parameters of the chosen electrolyte system

Cell parameters	Values obtained for 1 g GG + 1.2 M wt% of LiCl
1. Open circuit voltage (OCV)	1.88 V
2. Current	19 μA
3. Weight of the cathode	0.675 g
4. Weight of the anode	0.707 g
5. Weight of the electrolyte	0.147 g
6. Weight of the cell	1.529 g
7. Thickness of the cathode	1.423 mm
8. Thickness of the anode	1.569 mm
9. Area of the cell	1.82 cm^2
10. Discharge time	60 h
11. Current density	10.43 μA cm^{-2}
12. Power density	23.36 mW kg^{-1}

the conduction is mainly due to the cations and the calculated ionic transference number is 0.93 for the highest ion conducting membrane (1 g GG + 1.2 M wt% of LiCl). Cyclic voltammetry (CV) analysis was done to measure the cyclic stability of the prepared membrane which shows an adequate result by reciprocating the pattern for 50 cycles. Fabrication of Li-ion conducting primary battery has been optimized with an OCV of 1.88 V.

Declarations

References

1. Tarascon JM, Armand M (2011) Issues and challenges facing rechargeable lithium batteries. In: Materials for sustainable energy: a collection of peer-reviewed research and review articles from Nature Publishing Group, pp 171–179
2. Kumar LS, Selvin PC, Selvasekarapandian S, Manjuladevi R, Monisha S, Perumal P (2018) Tamarind seed polysaccharide biopolymer membrane for lithium-ion conducting battery. Ionics 24(12):3793–3803
3. Agrawal RC, Pandey GP (2008) Solid polymer electrolytes: materials designing and all-solid-state battery applications: an overview. J Phys D Appl Phys 41(22):223001
4. Chitra R, Sathya P, Selvasekarapandian S, Monisha S, Moniha V, Meyvel S (2019) Synthesis and characterization of iota-carrageenan solid biopolymer electrolytes for electrochemical applications. Ionics 25(5):2147–2157
5. Selvalakshmi S, Vijaya N, Selvasekarapandian S, Premalatha M (2017) Biopolymer agar-agar doped with NH4SCN as solid polymer electrolyte for electrochemical cell application. J Appl Polym Sci 134(15):44702 (1–10)
6. Kaplan DL (1998) Introduction to biopolymers from renewable resources. In: Biopolymers from renewable resources. Springer, Berlin, Heidelberg, pp 1–29

7. Selvin PC, Perumal P, Selvasekarapandian S, Monisha S, Boopathi G, Chandra ML (2018) Study of proton-conducting polymer electrolyte based on K-carrageenan and NH₄SCN for electrochemical devices. Ionics 24(11):3535–3542

8. Moniha V, Alagar M, Selvasekarapandian S, Sundaresan B, Hemalatha R, Boopathi G (2018) Synthesis and characterization of bio-polymer electrolyte based on iota-carrageenan with ammonium thiocyanate and its applications. J Solid State Electrochem 22(10):3209–3223

9. Khiar AA, Arof AK (2010) Conductivity studies of starch-based polymer electrolytes. Ionics 16(2):123–129

10. Monisha S, Selvasekarapandian S, Mathavan T, Benial AMF, Manoharan S, Karthikeyan S (2016) Preparation and characterization of biopolymer electrolyte based on cellulose acetate for potential applications in energy storage devices. J Mater Sci: Mater Electron 27(9):9314–9324

11. Rasali NMJ, Nagao Y, Samsudin AS (2019) Enhancement on amorphous phase in solid biopolymer electrolyte based alginate doped NH₄NO₃. Ionics 25(2):641–654

12. Muthukrishnan M, Shanthi C, Selvasekarapandian S, Manjuladevi R, Perumal P, Selvin PC (2019) Synthesis and characterization of pectin-based biopolymer electrolyte for electrochemical applications. Ionics 25(1):203–214

13. Singh R, Bhattacharya B, Rhee HW, Singh PK (2015) Solid gellan gum polymer electrolyte for energy application. Int J Hydrogen Energy 40(30):9365–9372

14. Noor IM (2020) Determination of charge carrier transport properties of gellan gum–lithium triflate solid polymer electrolyte from vibrational spectroscopy. High Perform Polym 32(2):168–174

15. Noor ISM, Majid SR, Arof AK, Djurado D, Neto SC, Pawlicka A (2012) Characteristics of gellan gum–LiCF3SO3 polymer electrolytes. Solid State Ionics 225:649–653

16. Neto MJ, Sentanin F, Esperança JMSS, Medeiros MJ, Pawlicka A, de Zea Bermudez V, Silva MM (2015) Gellan gum—Ionic liquid membranes for electrochromic device application. Solid State Ionics 274:64–70

17. Majid SR, Sabadini RC, Kanicki J, Pawlicka A (2014) Impedance analysis of gellan gum-poly (vinyl pyrrolidone) membranes. Mol Cryst Liq Cryst 604(1):84–95

18. Kumar GG, Munichandraiah N (2000) Effect of plasticizers on magnesium-poly (ethyleneoxide) polymer electrolyte. J Electroanal Chem 495(1):42–50

19. Chieng BW, Ibrahim NA, Yunus WMZW, Hussein MZ (2014) Poly (lactic acid)/poly (ethylene glycol) polymer nanocomposites: effects of graphene nanoplatelets. Polymers 6(1):93–104

20. Chandra MVL, Karthikeyan S, Selvasekarapandian S, Premalatha M, Monisha S (2017) Study of PVAc-PMMA-LiCl polymer blend electrolyte and the effect of plasticizer ethylene carbonate and nanofiller titania on PVAc-PMMA-LiCl polymer blend electrolyte. J Polym Eng 37(6):617–631

21. Naachiyar RM, Ragam M, Selvasekarapandian S, Krishna MV, Buvaneshwari P (2021) Development of biopolymer electrolyte membrane using Gellan gum biopolymer incorporated with NH₄SCN for electro-chemical application. Ionics 27(8):3415–3429

22. Hodge RM, Edward GH, Simon GP (1996) Water absorption and states of water in semicrystalline poly (vinyl alcohol) films. Polymer 37(8):1371–1376

23. Hong T, Yin JY, Nie SP, Xie MY (2021) Applications of infrared spectroscopy in polysaccharide structural analysis: progress, challenge and perspective. Food Chem: X 12:100168

24. Setyaningrum DL, Riyanto S, Rohman A (2013) Analysis of corn and soybean oils in red fruit oil using FTIR spectroscopy in combination with partial least square. Int Food Res J 20(4):1977

25. Cassanelli M, Norton I, Mills T (2017) Effect of alcohols on gellan gum gel structure: bridging the molecular level and the three-dimensional network. Food Struct 14:112–120

26. Halim NFA, Majid SR, Arof AK, Kajzar F, Pawlicka A (2012) Gellan gum-LiI gel polymer electrolytes. Mol Cryst Liq Cryst 554(1):232–238

27. Monisha S, Mathavan T, Selvasekarapandian S, Benial AMF (2017) Preparation and characterization of cellulose acetate and lithium nitrate for advanced electrochemical devices. Ionics 23(10):2697–2706

28. Vijaya N, Selvasekarapandian S, Hirankumar G, Karthikeyan S, Nithya H, Ramya CS, Prabu M (2012) Structural, vibrational, thermal, and conductivity studies on proton-conducting polymer electrolyte based on poly (N-vinylpyrrolidone). Ionics 18(1–2):91–99

29. Selvalakshmi S, Mathavan T, Selvasekarapandian S, Premalatha M (2019) Characterization of biodegradable solid polymer electrolyte system based on agar-NH₄Br and its comparison with NH 4 I. J Solid State Electrochem 23(6):1727–1737

30. Perumal P, Selvin PC, Selvasekarapandian S, Sivaraj P (2019) Structural and electrical properties of bio-polymer pectin with LiClO4 solid electrolytes for lithium ion polymer batteries. Mater Today: Proc 8:196–202

31. Boukamp BA (1986) A package for impedance/admittance data analysis. Solid State Ionics 18:136–140

32. Kumar LS, Selvin PC, Selvasekarapandian S (2021) Impact of lithium triflate (LiCF3SO3) salt on tamarind seed polysaccharide-based natural solid polymer electrolyte for application in electrochemical device. Polym Bull 78(4):1797–1819

33. Boopathi G, Pugalendhi S, Selvasekarapandian S, Premalatha M, Monisha S, Aristatil G (2017) Development of proton conducting biopolymer membrane based on agar–agar for fuel cell. Ionics 23(10):2781–2790

34. Nithya H, Selvasekarapandian S, Selvin PC, Kumar DA, Kawamura J (2012) Effect of propylene carbonate and dimethylformamide on ionic conductivity of P (ECH-EO) based polymer electrolyte. Electrochim Acta 66:110–120

35. Prodromakis T, Papavassiliou C (2009) Engineering the Maxwell-Wagner polarization effect. Appl Surf Sci 255(15):6989–6994

36. Mary IA, Selvanayagam S, Selvasekarapandian S, Chitra R, Chandra ML, Ponraj T (2020) Lithium ion conducting biopolymer membrane based on K-carrageenan with LiNO 3. Ionics 26(9):4311–4326

37. Hemalatha R, Alagar M, Selvasekarapandian S, Sundaresan B, Moniha V, Boopathi G, Selvin PC (2019) Preparation and characterization of proton-conducting polymer electrolyte based on PVA, amino acid proline, and NH4Cl and its applications to electrochemical devices. Ionics 25(1):141–154

38. Chitra R, Sathya P, Selvasekarapandian S, Meyvel S (2020) Synthesis and characterization of iota-carrageenan biopolymer electrolyte with lithium perchlorate and succinonitrile (plasticizer). Polym Bull 77(3):1555–1579

39. Selvasekarapandian S, Hema M, Kawamura J, Kamishima O, Baskaran R (2010) Characterization of PVA—NH4NO3 polymer electrolyte and its application in rechargeable proton battery. J Phys Soc Jpn 79:163–168

40. Genova FKM, Selvasekarapandian S, Karthikeyan S, Vijaya N, Pradeepa R, Sivadevi S (2015) Study on blend polymer (PVA-PAN) doped with lithium bromide. Polym Sci, Ser A 57(6):851–862

41. Premalatha M, Mathavan T, Selvasekarapandian S, Monisha S, Selvalakshmi S, Pandi DV (2017) Tamarind seed polysaccharide (TSP)-based Li-ion conducting membranes. Ionics 23(10):2677–2684